applied sciences

MDPI

Article

Optimum Driving of Ultrasonic Cleaner Using Impedance and FFT Analysis with Validation of Image Processing of Perforated Foils

Muhammad Usman Khan [1], Faisal Rehman [1], Mohsin Saleem [2,3], Hassan Elahi [1], Tae Hyun Sung [4] and Hamid Jabbar [1,*]

1 Department of Mechatronics Engineering, College of Electrical and Mechanical Engineering, National University of Sciences and Technology (NUST), H-12, Islamabad 44000, Pakistan
2 School of Chemical and Materials Engineering, National University of Sciences and Technology (NUST), H-12, Islamabad 44000, Pakistan
3 School of Interdisciplinary Engineering & Sciences, National University of Sciences and Technology (NUST), Islamabad 44000, Pakistan
4 Department of Electrical Engineering, Hanyang University, Seoul 04763, Republic of Korea
* Correspondence: hamid.jabbar@ceme.nust.edu.pk; Tel.: +92-300-5274026

Featured Application: Ultrasonic cleaners are widely used in the cleaning of surgical instruments, automobile parts, jewellery, fruits and vegetable, and in chemical synthesis.

Abstract: Over the past decade, ultrasonic cleaners have been widely used in many industries. Now, this technology is finding its way into homes for vegetable, fruit, and clothes cleaning. In widely used ultrasonic cleaners, piezoelectric transducers are externally attached to the steel tank to generate ultrasonic waves inside the tank. Based on the impedance data of the piezoelectric transducers, the driving circuit was tuned to generate the required frequencies inside the cleaning tank. This paper discusses the design, development, and validation of an 800 mL tank capacity ultrasonic cleaner driven with a piezoelectric disc actuator. To achieve an optimum cleaning action without surface abrasion, several characteristics need to be considered in this complex relationship. The placement of transducers has been investigated according to the pressure distribution inside the liquid medium. The optimized ultrasonic cleaner design, along with a class-D half-bridge circuit, was developed to drive the ultrasonic transducer in the resonance frequency range. To validate the optimal design and driving frequency, the acoustic spectrum generated inside the tank was measured using a piezoelectric sensor and FFT analysis was performed. To validate the cleaning effect, a qualitative test based on aluminium foil perforations was performed. The perforation area in the foils was quantitatively measured using image processing based on the YOLO V5 technique. The proposed image processing technique has an accuracy of 97% in the detection of perforation areas in the aluminium foil test.

Keywords: ultrasonic cleaner; piezoelectric; D-class inverter; YOLO V5; image processing

check for updates

Citation: Khan, M.U.; Rehman, F.; Saleem, M.; Elahi, H.; Sung, T.H.; Jabbar, H. Optimum Driving of Ultrasonic Cleaner Using Impedance and FFT Analysis with Validation of Image Processing of Perforated Foils. *Appl. Sci.* **2023**, *13*, 6991. https://doi.org/10.3390/app13126991

Academic Editor: Theodore E. Matikas

Received: 18 November 2022
Revised: 26 December 2022
Accepted: 11 January 2023
Published: 9 June 2023

1. Introduction

The ultrasonic cleaner is a device in which ultrasound waves are generated inside a liquid medium using an external source. This external source is usually a piezoelectric material-based transducer which generates ultrasonic frequency when powered by alternating voltage in its resonance frequency range. For decades, ultrasonic cleaners have been used in metallurgy, industrial manufacturing, textile, automotive industries, chemical laboratories, etc. Some common uses are cleaning glassware, jewellry, surgical instruments, automotive parts, teeth, and enhancing chemical reactivity. Apart from the technical aspect, the industry is now using ultrasonic cleaning for other advantages as well. These include a lesser cleaning time for the number of parts, more efficient cleaning as compared with conventional cleaning, increased productivity, and decreased cost of materials. New applications of ultrasonic cleaners are in fruit, vegetable, and clothes cleaning at home [1].

Ultrasonic waves generated inside the cleaners are differentiated based on their application, power, and frequency [2]. There are different types of transducers which are used to generate ultrasonic waves inside an ultrasonic cleaner, which include Bolt-clamped Langevin (BLT), piezoelectric ceramic (Lead Zirconate Titanate or PZT) disc, and magnetostrictive-based transducers [3]. Electromagnetic transducers can also generate ultrasonic frequencies, but the most widely used are the piezoelectric transducers in ultrasonic cleaning. Piezoelectric-based ultrasonic transducers have a slight advantage in terms of small size, no noise, higher efficiency, and non-flammable over electromagnetic-based ultrasonic transducers [4].

Piezoelectric transducers are used to convert alternating electrical energy into ultrasonic acoustic waves inside the steel tank of ultrasonic cleaners [5]. The negative phase of these waves will create small bubbles and the positive phase results in bubble collapse, creating very high local pressure and temperature [6]. With the help of high-amplitude acoustic waves, a pressure tension change is induced inside the liquid medium (or cleaning solvent). A result of this pressure tension change is cavitation, which is the formation of bubbles at the microscopic level that grow and then explode. This explosion of bubbles will remove particles (soils or adulterants) from the cleaning object's surface [7].

There are different types of ultrasonic cleaners available in the market. They can be differentiated based on their size, power, the number of transducers and their placement. In this research, the design and development of an ultrasonic cleaner have been carried out for optimum performance, and the design is validated using a proposed image-based efficiency measurement technique. This work is an effort to combine the design, tuning, and validation of the piezoelectric transducer-based ultrasonic cleaner.

To design an ultrasonic cleaner, acoustic simulations need to be performed to optimize design parameters such as size, the number of transducers and their location [8,9]. In COMSOL Multiphysics, we have performed acoustic simulations of the tank to determine the pressure distributions of various designs. In an optimum tank design, the number and location of the transducers were determined based on these simulations.

Piezoelectric transducer resonance frequency varies with the diameter. The generated ultrasonic wave power depends on the thickness and layer of the piezoelectric disc [10,11]. Commercially available piezoelectric discs and BLT transducers have different thicknesses and diameters based on the required cleaning frequency. First, a 40 kHz transducer was chosen for general cleaning applications, and impedance analysis of transducers was performed to determine their resonant and anti-resonant points by using an impedance-frequency graph [12,13]. Based on these impedance graphs, transducer driving circuitry was designed.

A piezoelectric transducer driving circuit is developed using a D-class inverter [14,15]. The circuit considers different parameters such as ease of control, high power output, and variable frequency (so that different types of transducers can be actuated using a single circuit). To test and tune the driving circuit, piezoelectric disc sensors (similar to hydrophones) were used to acquire ultrasonic wave data inside the liquid tank [16]. These hydrophones are used here to acquire the frequency response inside the liquid medium. An FFT was performed on the time domain sensor voltage output to analyze the ultrasonic waves generated between anti-resonance and resonance peaks.

Ultrasonic cleaners are widely used, but challenges remain in the determination of their optimum working frequency and cleaning efficiency. To efficiently operate the ultrasonic cleaner and its operating frequency, the voltage should be optimally selected. In [16], researchers used a coated quartz crystal sensor to detect the movement of ultrasonic waves inside the ultrasonic cleaning tank. This frequency output can be used as feedback to optimally drive or tune the ultrasonic transducer.

Cavitation is responsible for cleaning in ultrasonic cleaners [17]. There are several methods to measure and detect cavitation. These methods include the foil corrosion test [18,19], detecting cavitation with the help of hydrophone [20], portable cavitation meter [21,22], optical methods [23], and particle counters [23]. Cavitation causes the pitting of metal surfaces; therefore, ordinary aluminuim kitchen foil is commonly used to test the working efficiency of ultrasonic cleaners. In ordinary kitchen foil, this pitting becomes perforations [24]. The efficiency of ultrasonic cleaners depends on the size and number of cavitation bubbles, temperature, viscosity, surface tension, and diffusion rate of the liquid [1]. For this research, an aluminuim foil corrosion test was performed in room conditions. After placing the foils in powered ultrasonic cleaner tanks, the corrosion area of the foil due to perforation was then measured using image processing and converted into quantifiable results.

The main objectives of this paper are to combine the design, tuning and validation of ultrasonic cleaners as follows: (1) to design (placement and the number of ultrasonic transducers) an ultrasonic cleaner based on the acoustic pressure distribution of the system in a simulation environment, (2) to provide a gateway for how to design a driving circuit for ultrasonic transducers based on the results of the impedance analysis of the transducer, (3) to tune the system using replicated hydrophone technique so that we can have quantifiable results whether the ultrasonic cleaner is working in the resonance region or not, (4) to provide a generic validation method for finding the efficiency of ultrasonic cleaners easily, effectively, and cheaply.

This paper is organized as follows; in Section 2, a detailed methodology is discussed. Section 3 includes a discussion on design parameters, boundary conditions, and acoustic simulation, which are pre-requisite for the mechanical design of an ultrasonic cleaner. Finally, experimental setup, testing, and results are shown in Section 4 of this paper followed by the discussion in Section 5 and the conclusion in Section 6.

2. Ultrasonic Cleaner Design Methodology

The ultrasonic cleaner design methodology and process are presented in Figure 1, which also gives an overview of the structure of the research. The research has been divided into three parts. The first step in developing an ultrasonic cleaner was to find the optimum number and location of the transducer placement. Different tank sizes were available, for this study we selected a stainless-steel tank of 800 mL capacity, as it was readily available in the market. The COMSOL Multiphysics, FEM software tool was used for acoustic simulation. By using acoustic simulations, six different designs were evaluated based on pressure distribution. One design was selected, based on the number and placement of ultrasonic transducers. The selected design was manufactured, and a driving circuit was fabricated.

To validate the frequencies generated inside the tank and to optimize the driving frequency, piezoelectric disc sensors were used to acquire the frequencies generated inside the water-filled tank in the second phase of this research work. An oscilloscope was used to obtain the time domain signal of these piezoelectric disc sensors, which was then converted into a frequency domain signal by using FFT in MATLAB. This experimental campaign was necessary to find the behaviour of the circuit, ultrasonic transducers, and waves induced inside the ultrasonic tank.

In the third phase of this work, validation for this system was developed. For this purpose, an aluminuim foil corrosion test combined with image processing is presented. A total of 100 images were acquired for this purpose, and different image processing techniques such as segmentation and thresholding were applied to obtain quantitative results. The main purpose behind this phase was to find the perforation area in aluminuim foils. The comparison of perforation areas in aluminuim foil at different locations inside the tank, operating times, and transducer power can be used to compare different ultrasonic cleaners and to identify the problem and tuning-related issues.

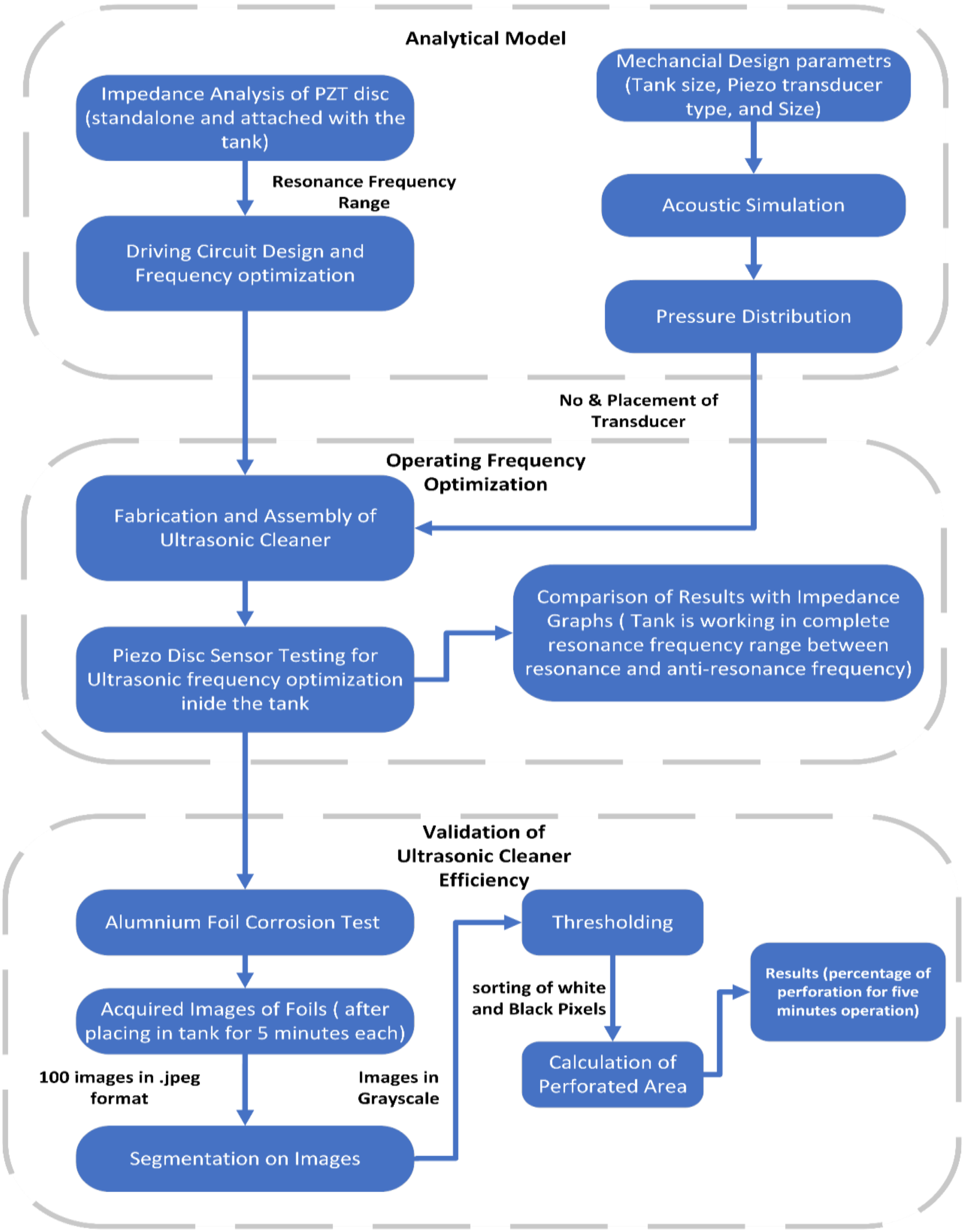

Figure 1. Block Diagram of Proposed Methodology.

This system was proposed to provide a generic pathway for the upcoming researchers, as the literature cited shows that there are many articles which used the concept of foil corrosion tests, but none presented a systematic way of finding and evaluating these perforations quantitatively. So, we propose a system which can obtain a quantitative result of perforation in terms of the perforation area of the foil. For the proposed image processing system, the user does not need to care about the image pixels, surrounding environments, or dimensions of the foils as it is a generic system, as explained in the later sections.

2.1. Ultrasonic Transducer Driving Circuit

This research was proposed to design an ultrasonic cleaning machine and its driving electronics model after a comprehensive review of the design, fabrication, and driving techniques for the ultrasonic cleaning machine. We proposed the Class-D Inverter topology [25] to drive the Ultrasonics transducer with high frequency for ultrasonic waves, as shown in Figure 2. The proposed Electronics circuit model is divided into three parts. The first part converts the main supply voltage to DC-Link voltage. The second part generates the controllable 40 kHz frequency to drive the piezoelectric transducer for generating the ultrasonic waves.

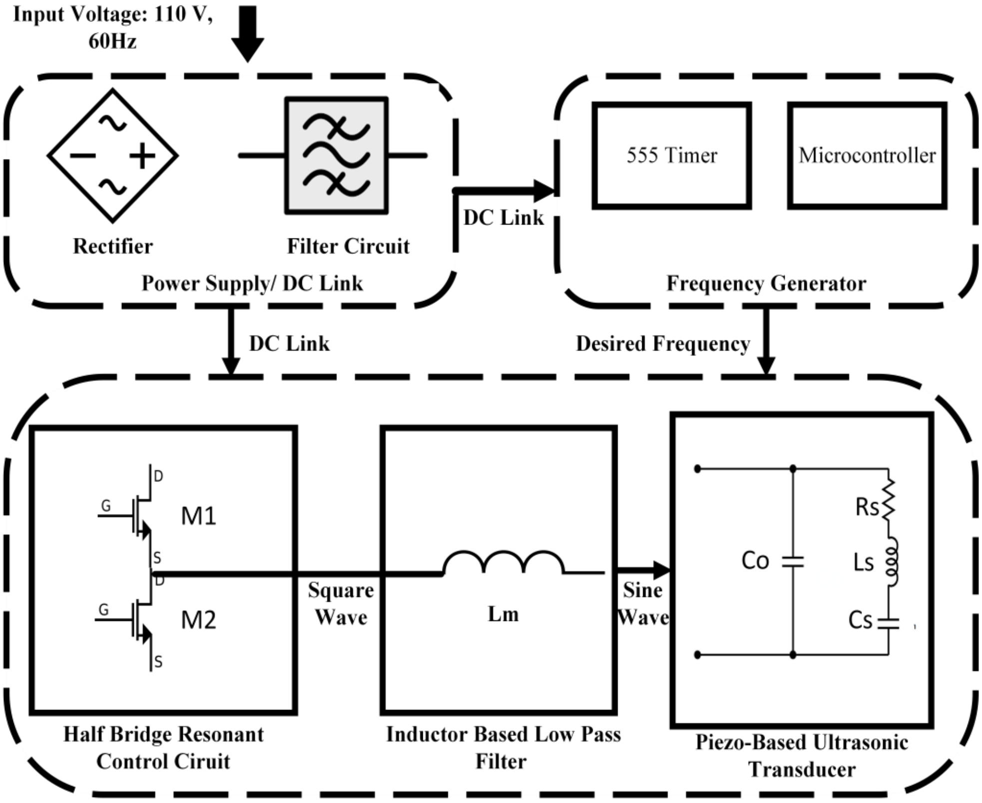

Figure 2. Proposed System Block Diagram.

To drive the piezoelectric transducer in the ultrasonic cleaner, the square wave voltage signal generated by the class-D inverter works with an LC resonant circuit to generate a sine wave voltage signal [26]. The piezoelectric disc static capacitance (C_o) works in resonance with the inductor (L_s) as a low-pass filter to generate a sine wave signal. The values in Table 1 were used for the equivalent model of the proposed scheme.

$$Fs = \frac{1}{2\pi\sqrt{LC}} \quad (1)$$

Table 1. Electrical Properties of D Class Inverter.

Electrical Components		Operating Values
Input Dc-Link Voltage	V_{in}	170 V
Maximum Output Power of Circuit	P_m	50 W
Maximum Current	I_m	100 mA
Maximum Output Voltage	V_o	840 V
Magnetizing Inductor	L_m	1.0 mH
Switching Frequency	F_s	40 KHz (range)
MOSFET Model	M1 and M2	6N80
Piezo Capacitance	C_o	8.35 nF
PZT Resistance	R_p	310 Ω
PZT Disc Diameter	mm	50 mm
PZT Disc Thickness	mm	2.5 mm
PZT Material	-	PZT-4A
PZT Electrode Printing Type		Wrap Around Feedback
PZT Disc Power	watt	35 W

Table 1 shows the electronic parameters for the UCT driving machine, and the piezo disc parameters. The proposed circuit was designed for a maximum power output of 50 W and a maximum current of 100 mA. The magnetizing inductor is the core element to adjust the transducer input voltage and current capacity (to get 35 W of power). As the piezoelectric disc is made of Hard piezoelectric ceramic (PZT-4A), the driving voltage can be set to a maximum value of about 750 V, which corresponds to 300 V/mm and is in a safe range to not cause de-poling and excess heating.

3. Acoustic Simulation

While working with ultrasonic cleaning acoustic effects are very important, as these effects are responsible for the induced shear forces inside the ultrasonic cleaner (UC). These shear forces are responsible for generating cavitation inside of the ultrasonic tanks [27,28]. For this research, acoustic simulation was carried out in COMSOL Multiphysics. There are six different UC designs, with different numbers and placement of ultrasonic transducers used.

3.1. Design Consideration

A 2D acoustic simulation was carried out for this work. A tank with dimensions 140 mm × 140 mm × 152 mm (L × W × D) was simulated in FEM software COMSOL Multiphysics as shown in Figure 3. The internal body of the geometry was selected as water (liquid medium) and the external boundary was selected as stainless steel type 308 (tank of cleaner). The sole purpose of selecting all of these parameters is that we had a stainless steel container with water as a liquid medium inside it, which had already been selected and developed for this research work.

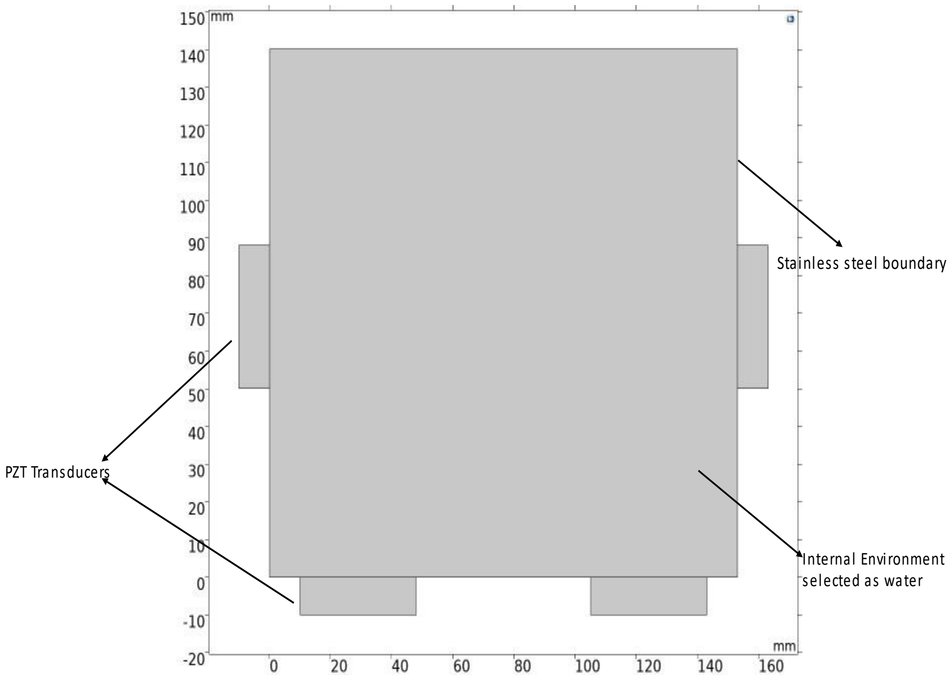

Figure 3. Dimension and Material Selection in COMSOL Multiphysics.

3.2. Boundary Conditions

Six different designs were considered for simulations having different numbers and placement of transducers. The boundary conditions were kept the same for all of the designs/models. These boundary conditions are shown in Table 2.

Table 2. Boundary Conditions for Acoustic Simulation.

Boundary Condition	Selected at	Reason/Comment
Sound Hard Boundary	All of the boundaries except the top of the container (which is open), and the contact point of the container and the PZT Disc	To avoid any external interference of waves.
Plane Wave Radiation	Selected on top of the tank only.	To allow the waves to leave the system with a minimal angle of reflection.
Exterior Field Calculations	Selected on top of the tank only	Selected for scattered boundaries and waves.

3.2.1. Comparison of Different Designs of Ultrasonic Cleaner

Six different ultrasonic cleaner designs were simulated to find the optimum design. According to the acoustic simulation results, a design developing the best results (both in terms of pressure distribution and electrical energy consumption) was selected.

In Figure 4, six different design models and pressure distribution results are shown. These results show positive–negative pressure change (or pressure–tension change) in the tank along with their intensity. From the simulations, the following conclusions were drawn for optimum design selection.

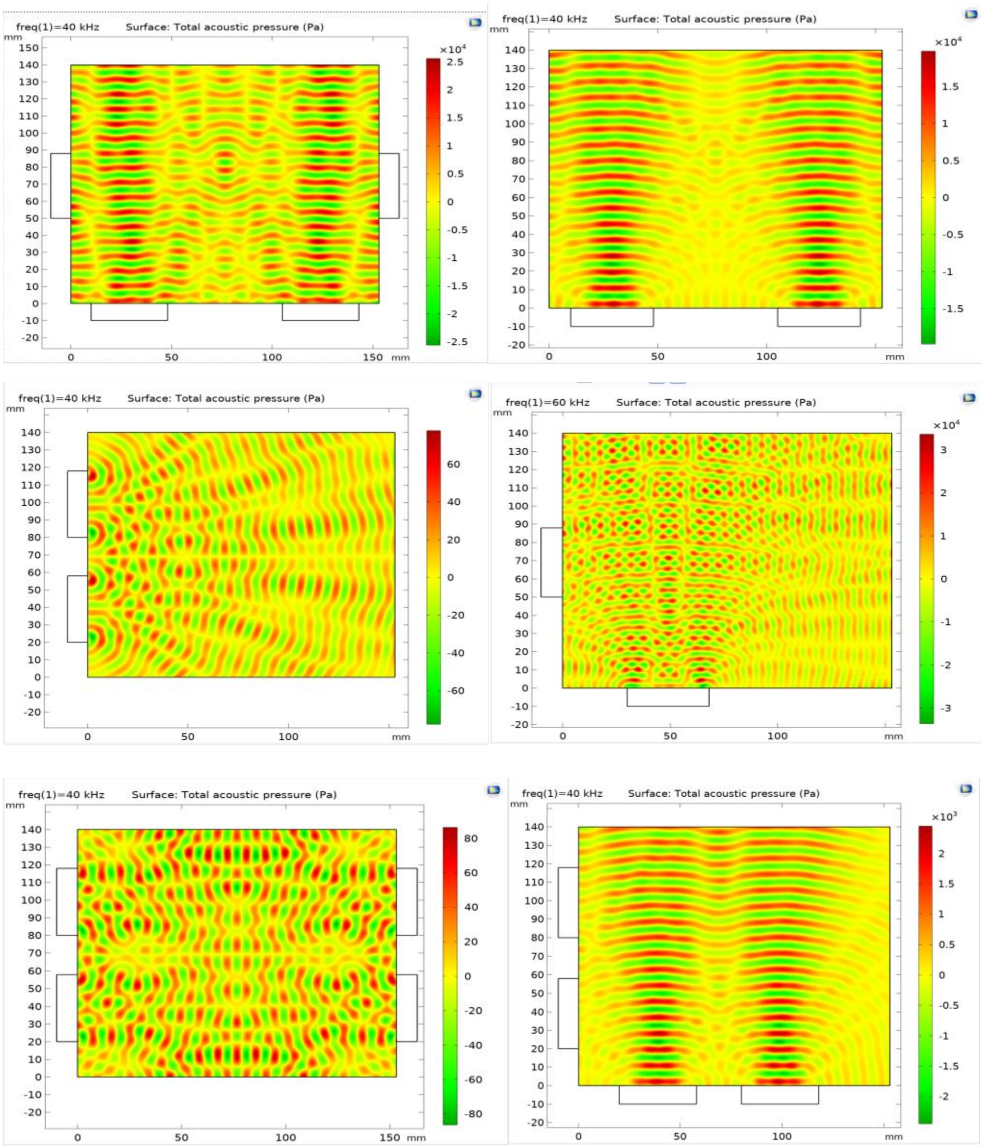

Figure 4. Six Different design models with FEM Acoustic Simulation.

1. Models c and e cannot be selected, as the intensity of pressure distribution values are very low;
2. In model d, the pressure is dense near the transducers and lower when away from transducers;
3. In models a and f, four transducers were used, which resulted in higher electrical energy consumption than in model b, which used only two transducers but produced the same pressure distribution and acoustic response;
4. Model b was selected and replicated for this research work.
5. For efficient cleaning, there is also a requirement of height distance from the transducer to the bottom tip of the cleaning object; therefore, a basket was used in an ultrasonic cleaner to provide the optimum height. By achieving this optimum height, better cleaning can be achieved.

3.3. Fabrication of Ultrasonic Cleaner

Model b from Figure 4 was selected as optimum from the results of the FEM acoustic simulation. The model has been replicated, and an outer body of the ultrasonic cleaner has been manufactured with the help of stainless-steel material (308). The body of the cleaner contains a timer, LED indicators, and hot air vents. A labelled figure of ultrasonic cleaner is shown in Figure 5.

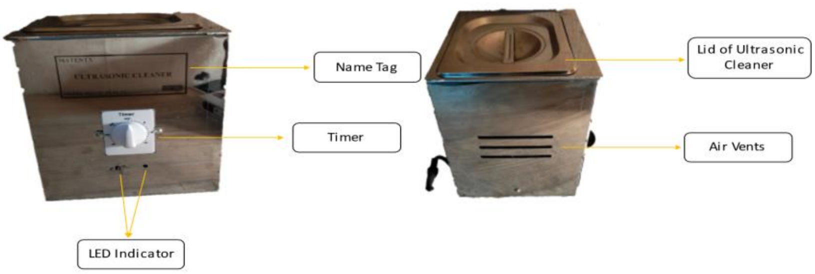

Figure 5. Fabricated Ultrasonic Cleaner.

Internal Structure and Transducers Placement

Transducer placement was determined using FEM acoustic simulation. From Section 3.2.1, the location of the transducer (PZT disc) was identified. The results show that the transducer gave the best performance when attached to the bottom of the tank. For simulations, two stacked piezoelectric discs were used; the reason behind this configuration is to produce maximum ultrasonic waves which can create more pressure–tension change in the simulation. For experimental design. a single disc that was 2.5 mm thick with a diameter of 50 mm was used. The attached PZT with the tank is shown in Figure 6. The size of the tank used for this research work is 140 mm × 140 × 152 mm (L × W × D). The piezo disc details are listed in Table 1. The PZT disc was attached to the container using general epoxy (available as steel epoxy in the market). Epoxy was applied only at the corner of the PZT disc. The FR4 material was placed between the PZT disc and the steel tank.

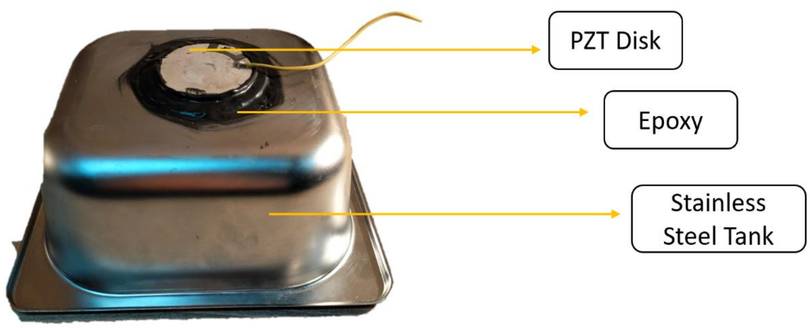

Figure 6. Ultrasonic Tank with PZT Disk (Ultrasonic Transducers).

4. Experimental Section

Different experiments for finding the accuracy of the ultrasonic cleaner were performed on the designed ultrasonic cleaner. Two different experimental techniques were used for this research. One is an FFT analysis using a replicated hydrophone (PZT buzzer disc), and the other is Image processing validation (foil corrosion test).

4.1. Experimental Setup

The experimental setup for the FFT Analysis and foil corrosion test is shown in Figures 7 and 8, respectively. The setup shown in Figure 7 has an ultrasonic cleaner, which is used to agitate a liquid medium with the help of which ultrasonic waves will generate inside it. A piezoelectric buzzer disc (acting as a low-cost hydrophone) was used here to measure the amplitude of ultrasonic waves being induced inside of the liquid medium of the ultrasonic tank. In ultrasonic cleaning, hydrophones are used to find acoustic pressure distribution at different frequency points in a frequency spectrum [29]. Different types of hydrophones are available in the market, and the choice of hydrophone depends on the frequency of the ultrasonic cleaner [30]. An oscilloscope was utilized for obtaining the wave response in the time domain. The sample size of the oscilloscope was set at 100 KS/s (kilo samples per second). According to the Nyquist Theorem states, the sample size must be at least double the size of the maximum frequency (40 kHz in this case) being induced in the system. To hold the piezoelectric buzzer disc firm inside the ultrasonic cleaning tank a magnetic stand was used, as shown in Figure 7.

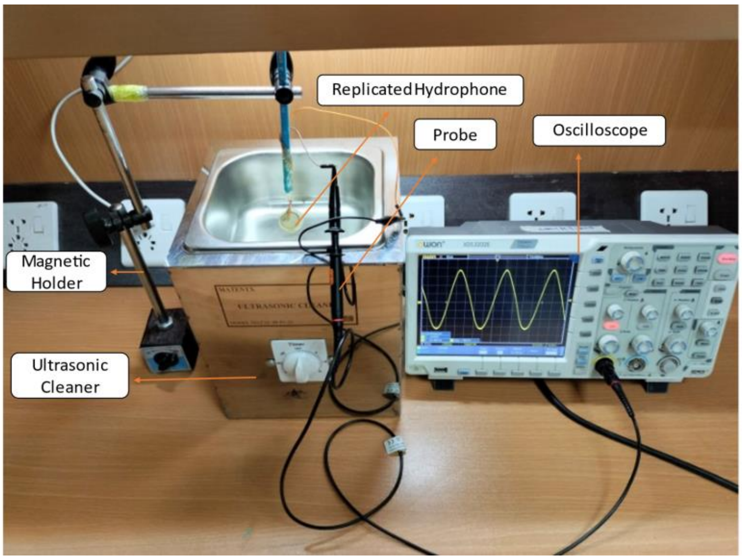

Figure 7. FFT Analysis using Replicated Hydrophone.

For the second experimental campaign, i.e., foil corrosion tests, an experimental setup was designed that consisted of two parts, as shown in Figures 8 and 9. The setup shown in Figure 8 is used for obtaining corroded aluminuim foils. A large number of aluminuim foils (100 in number) were dipped inside of the liquid medium in which ultrasonic waves were produced. These foils were dipped one by one, and the ultrasonic cleaner was operated for 5 min for each cycle. In the end, 100 perforated foils were obtained.

For the second part of this experiment, the 100 perforated aluminuim foil images were captured, and a dataset of 100 images was obtained. For obtaining the images of these foils, a uniform background, lighting conditions and the height of the camera were fixed as shown in the image acquisition setup in Figure 9. This setup depicts a stand made for providing the uniform height of the camera to aluminuim foil (i.e., 13 cm), a black sheet for providing proper background. An Infinix HOT10i camera (720 × 1600 pixels) was used with a bulb for proper lighting conditions. This setup is for experimental purposes, the results show that these parameters did not affect the results when the researchers or scientists used the system proposed in this article.

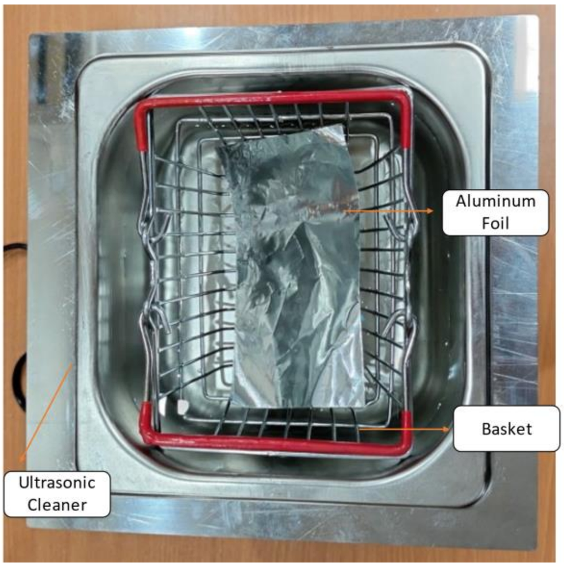

Figure 8. Aluminuim Foil Corrosion Test.

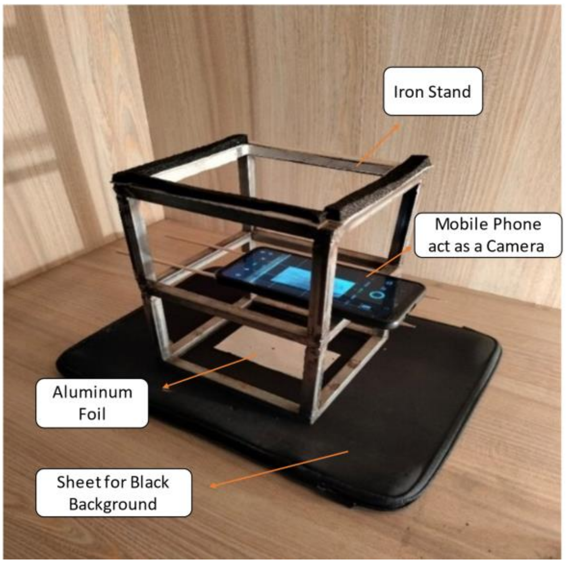

Figure 9. Image Acquisition Setup.

4.2. Testing and Results

Using a Piezoelectric disc as a hydrophone and obtaining a frequency domain signal will tell us about the amplitude of the frequencies in the agitated liquid medium. As discussed in the previous section; i.e., Section 4.1., different diameter piezoelectric discs were dipped inside of the liquid medium, and their related response was obtained with the help of an oscilloscope. The oscilloscope time domain signal was converted into a frequency domain signal using MATLAB, and the behaviour of the waves induced inside of the system was observed. An FFT response of the system is shown in Figure 10; the graphs show that other frequencies are negligible as compared with the driving frequency inside the tank.

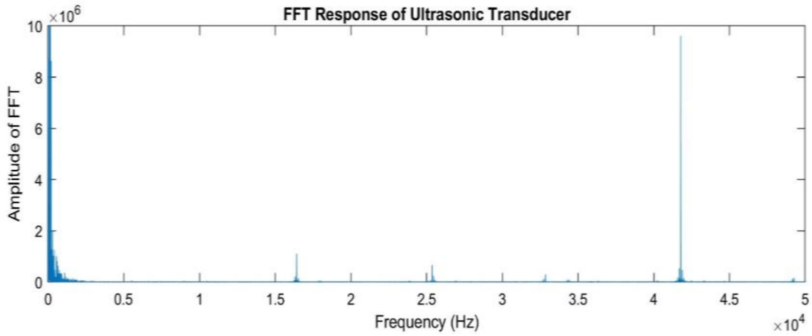

Figure 10. The frequency response of the Ultrasonic Cleaner, obtained at a single operating frequency (42 kHz) using Hydrophone.

To efficiently drive the ultrasonic cleaner, a pulsed driving circuit is required, as explained by [31]. To achieve pulse driving, a small DC link capacitor of value (1 uF/400 V) was used, and the FFT result obtained inside of the tank is shown in Figure 11.

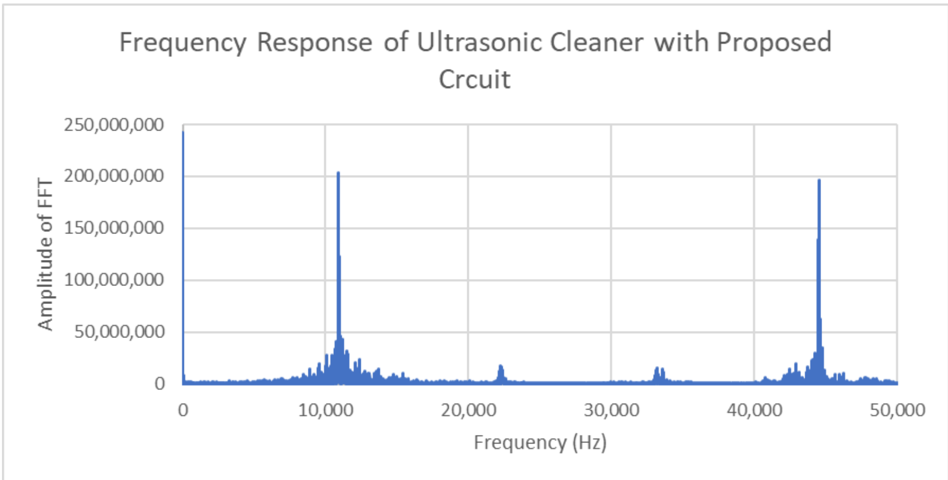

Figure 11. Frequency Response of Ultrasonic Cleaner using Proposed Circuit.

Artificial intelligence has been widely used to find the ultrasonic cleaner's efficiency. Zhong et al. [32], proposed a back propagation artificial neural network (BPANN) to find the material removal from an object that has been cleaned using ultrasonic cleaning. For the second series of experiments, a similar approach was used to find the efficiency of ultrasonic cleaning. For this purpose, a total of 100 images of aluminuim foils were taken. These 100 images were then augmented with gaussian noise, contrast, and brightness. After the augmentations, the total number of images in the dataset reached 300. These images were then labelled using labelling software with two different class labels; for premature perforation "low" label was assigned, and a "high" label was assigned to mature perforations. The dataset was then trained on YOLOv5 using Google Collaborate, which is an online cloud computing system which provides access to free GPUs. The overall results obtained using YOLOv5 models were not satisfactory. The best results were obtained using (YOLO v5s) weights, which are shown in Table 3.

Table 3. Precision and Recall of different Labels.

Sr no.	Class	Labels	Precision	Recall	mAP 0.5	mAP 0.5:0.95
1	All	272	0.445	0.562	0.527	0.231
2	High	156	0.565	0.891	0.869	0.415
3	Low	116	0.326	0.233	0.185	0.0475

Due to less accurate results, the above technique was terminated and another approach was adopted. For this approach python, open cv, was used for image processing. The dataset was the same as what was used for the YOLO V5 work. A GUI was also introduced for this purpose as shown in Figure 12. The user must upload the corroded foil image to the GUI and input the size of the foil in mm. The designed software then calculated the pixels of the image. With the size of an image, as provided by the user and the image pixel read by the software from the file, the software then calculates the total image area and pixel per square mm. A GUI is shown in Figure 13 along with all of the results of the image. The image was then converted into grayscale as shown in Figure 14, and thresholding was applied; i.e., the pixels having values less than 127 were termed as perforated pixels and others were termed as non-perforated pixels. In this way, the software calculated the perforated and non-perforated pixels. Then. by having the ratio of the perforated and non-perforated pixels available, the percentage of complete perforation in the foil was obtained.

Figure 12. Aluminuim Foil of Dimensions (120 mm × 120 mm).

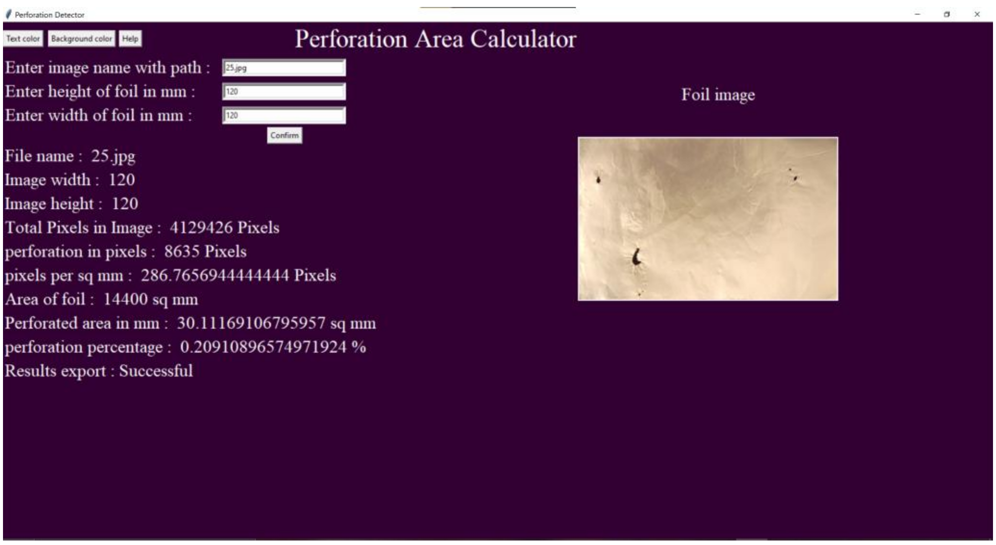

Figure 13. GUI for proposed system and Results.

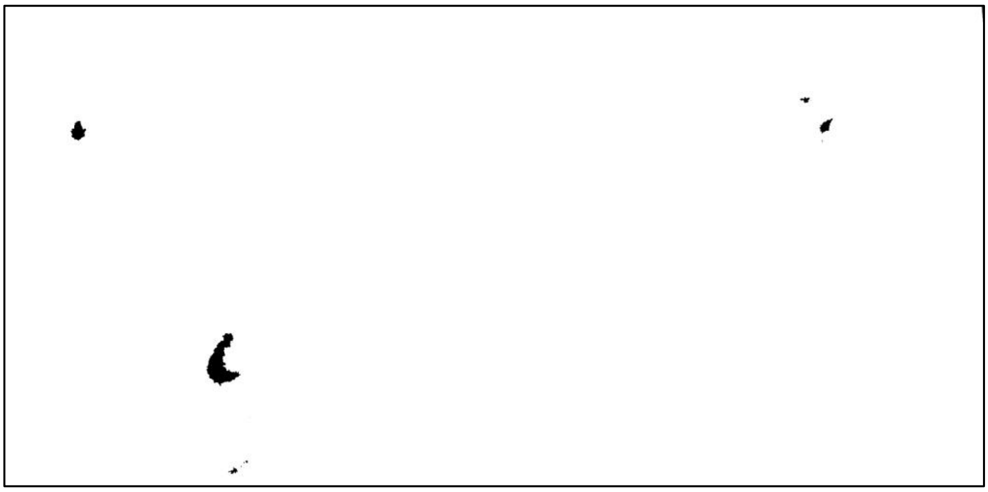

Figure 14. Converted Gray Scale Image.

A perforated aluminuim foil is shown in Figure 12. Later on, this image was exported to our GUI, which is the "Perforation Area Calculator", with the help of which one can obtain the perforation of the aluminuim foil. This perforation is obtained from the number of pixels of the image and dimensions of the foil (provided by the user, so that if a user uses a foil of different dimension the software adjusts itself accordingly).

The designed software also exported the results in the form of a text file which includes the overall size of the image, perforation per pixel, perforation per square mm, and perforation percentage. This technique has the following attributes; (1) any size of foil can be tested using this software, (2) the results obtained are accurate because the calculations work according to the number of pixels and size of the foil, (3) the results are independent of the lightning conditions, (4) a low-cost technique to check the validity of the ultrasonic cleaner.

5. Discussion

The proposed design of the ultrasonic cleaner was validated using two different techniques (replicated hydrophone and foil corrosion using image processing). The first technique (i.e., FFT results) was used to find the frequency response of the ultrasonic cleaner in running conditions. To obtain the optimum efficiency of a piezoelectric disc, the disc should have operated in the resonance region [33]. The results obtained from the FFT experimental campaign shows that the system has pulsating, driving DC voltage. The other peaks that can be observed in the FFT graphs inform us about the presence of other noises in the ultrasonic waves such as cavitation, external disturbance, and some small particles already present in the water.

Other technique will tell the user about the efficiency of the cleaner. The foil corrosion test has been an efficient technique for measuring the efficiency of the ultrasonic cleaner. For this research, image processing was introduced to the foil corrosion test to measure the corrosion area of a foil. Tangsopha et al. [20], have also implemented this technique. In this paper, the authors compared the results with the acoustic simulation in Ansys. In the same way, Yuan et al. [34], have also proposed image processing with a foil corrosion test. The results of these papers are improved, as the picture quality was low compared to this research. Also, they did not measure the perforation pixel by pixel, so the quantitative enhancement of the technique was also performed in this paper.

Table 4 shows the comparison between different works related to our proposed technique.

From Table 4, it can be observed that acoustic simulations were used either theoretically or for the behaviour at the contact point of the ultrasonic actuator and the ultrasonic cleaning tank. In this paper, we have used acoustic simulation to find the pressure distribution of acoustic waves when the number and placement of ultrasonic transducers have changed. The FFT section of this research shows the comparison of the harmonic frequency of the ultrasonic transducer with the frequencies induced inside of the cleaning tank. For this purpose, we have tuned our circuit accordingly, as mentioned in Section 2.1.

Table 4. Comparison of different techniques in Literature.

Refs.	Acoustic Simulation	FFT	Foil Corrosion Test
[35]	Theoretical application of acoustic in an ultrasonic cleaner. The analysis was performed only at the contact point.	FFT analysis was used here to find the magnitude of velocity in the x, y, and z direction	-
[20]	An acoustic simulation has been done for this paper to find the pressure distribution points inside the tank.	-	The pressure distribution points were thus verified using foil corrosion tests
[9]	To validate the concept of acoustic pressure with different parameters such as the volume of liquid, the thickness of the tank sheet, and the material properties of the tank.	-	This work was validated using a foil corrosion test.
[36]	The concept of acoustic simulation has not been done directly for this work, but they have introduced the concept of harmonic response analysis of fluid inside an ultrasonic cleaning tank.		A foil corrosion test was used to validate the results of the Harmonic Response Analysis.
[37]	-	-	Aluminuim foil corrosion test was used to compare temperature, nature of the solvent, and cleaning time and how these factors depend on the cleaning efficiency.

As observed in the literature, the technique of using aluminuim foil corrosion to find the efficiency of ultrasonic cleaning is not new. The only flaw we observed is that for foil corrosion there is no quantitative measurement method which tells us about the percentage area of the total perforation of the aluminuim foil when dipped inside of the running ultrasonic cleaner. For this purpose, we have designed a system in which the researcher, scientist, or worker does not need a specific dimension of foil, camera pixels, or lightning condition as this system worked on the distribution of black and white pixels. To validate this, consider the following aluminuim foils. These aluminuim foils have different dimensions (120 mm × 30 mm) and (60 mm × 60 mm), respectively, and their lighting condition and pixel ratios are also different. The results of these images are shown in the next figures (i.e., from Figures 15–18) respectively.

Figure 15. Aluminuim Foil having Dimension (120 mm × 30 mm).

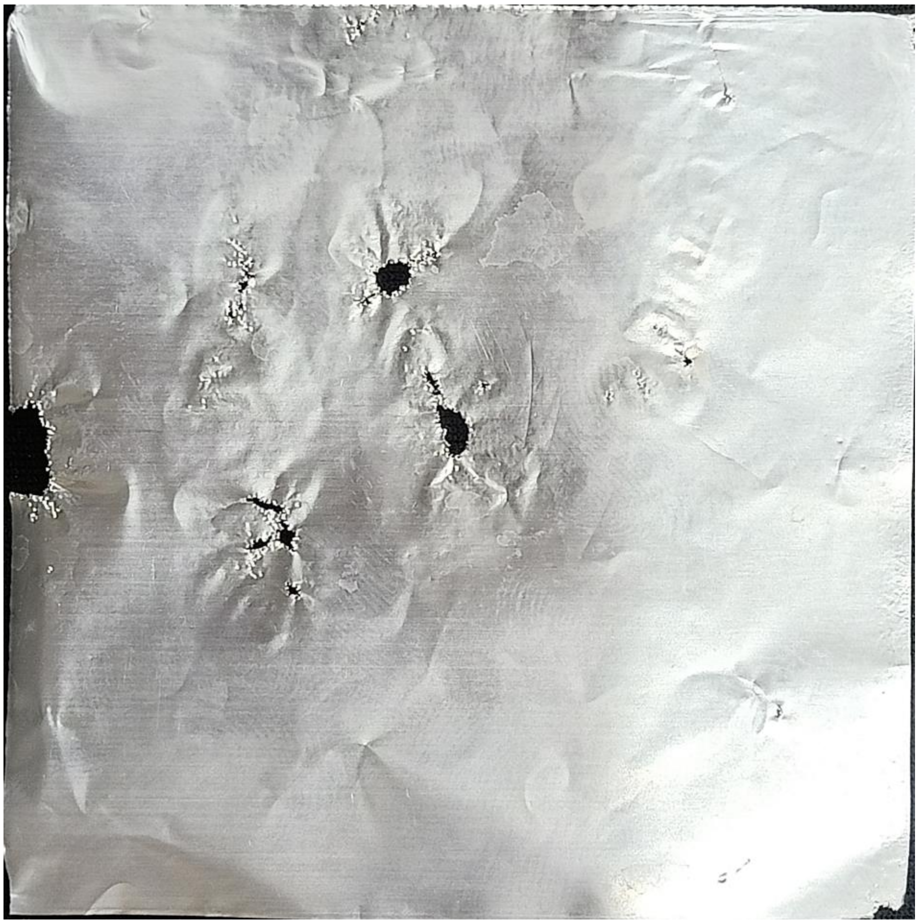

Figure 16. Aluminuim Foil having Dimension (60 mm × 60 mm).

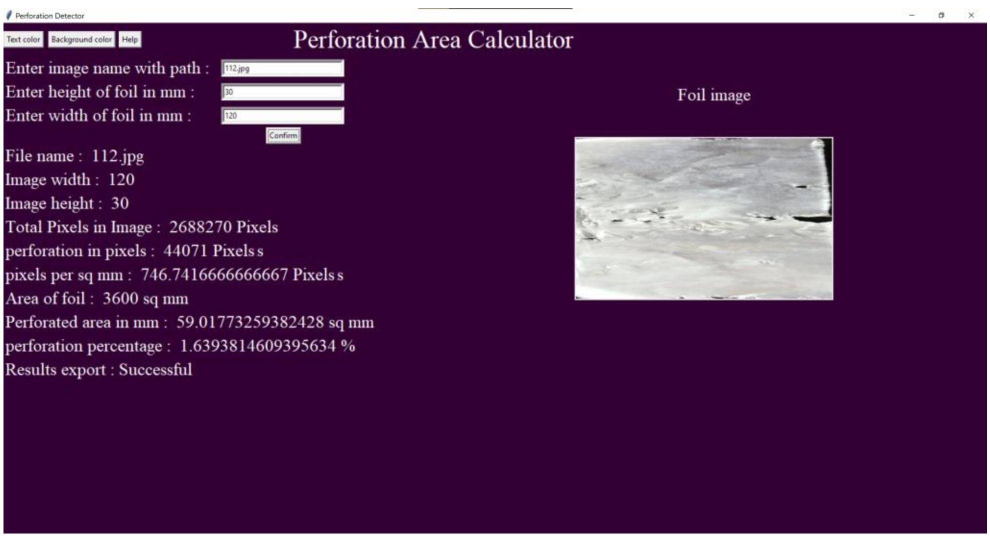

Figure 17. Results of Aluminuim Foil having Dimension (120 mm × 60 mm).

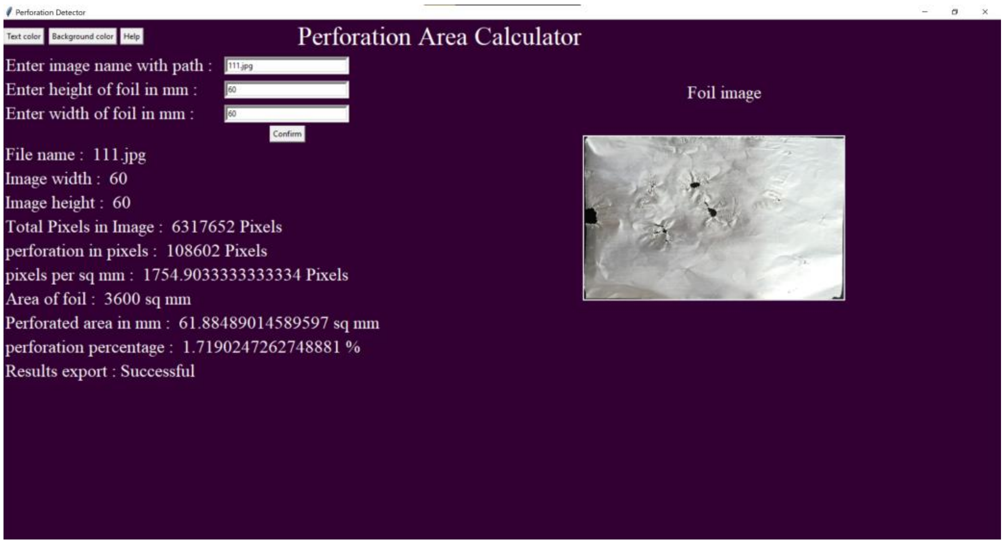

Figure 18. Results of Aluminuim Foil having Dimension (30 mm × 30 mm).

6. Conclusions

Ultrasonic cleaners have been widely used in different industries; they have played their role in cleaning small metals to large automobile parts, and cleaning small jewelry to large clothing items. In this work, the design methodology of an ultrasonic cleaner based on acoustic simulation in COMSOL Multiphysics was proposed. The designed cleaner was fabricated, and different experiments were performed. The transducer used was the PZT disc, which is responsible for generating ultrasonic waves inside of the liquid medium. To validate the efficiency of both transducers and ultrasonic cleaners, two different approaches have been presented. The first approach is the low-cost hydrophone approach, which was selected to validate whether the transducer was working in resonance mode and how much noise was present. With the help of this technique, the driving circuit's efficiency could also be confirmed. The second approach used was an image processing technique on corroded aluminuim foils. In this way, the efficiency of any ultrasonic cleaner can be obtained. These two techniques are low-cost compared with other techniques for measuring and quantifying cavitation inside of the ultrasonic cleaner.

Author Contributions: Conceptualization, M.U.K.; Methodology, F.R.; Formal analysis, T.H.S.; Investigation, M.S.; Resources, H.J.; Writing—original draft, H.E. All authors have read and agreed to the published version of the manuscript.

Funding: This work was jointly supported by the Pakistan's National Center of Robotics and Automation (NCRA) research fund "Indigenous Approach for Development of Piezoelectric Devices" (RF-NCRA-035), 2020, and HEC-NRPU research fund "Development of lab/pilot scale facilities for the production of piezoelectric material for multilayer energy devices" 20-15673/NRPU/R&D/HEC/2021.

Institutional Review Board Statement: Not applicable.

Informed Consent Statement: Not applicable.

Conflicts of Interest: The authors declare no conflict of interest.

References

1. Fuchs, F.J. Ultrasonic cleaning and washing of surfaces. In *Power Ultrasonics: Applications of High-Intensity Ultrasound*; Woodhead Publishing: Sawston, UK, 2015; pp. 577–609. [CrossRef]
2. Chobin, N. Surgical Instrument Decontamination: A Multistep Process. *AORN J.* **2019**, *110*, 253–262. [CrossRef] [PubMed]
3. Zhou, H.; Zhang, J.; Feng, P.; Yu, D.; Wu, Z. An amplitude prediction model for a giant magnetostrictive ultrasonic transducer. *Ultrasonics* **2020**, *108*, 106017. [CrossRef] [PubMed]
4. Uchino, K. Piezoelectric actuators 2006. *J. Electroceram.* **2008**, *20*, 301–311. [CrossRef]
5. Elahi, H.; Eugeni, M.; Gaudenzi, P. *Piezoelectric Aeroelastic Energy Harvesting*; Elsevier: Amsterdam, The Netherlands, 2021.

6. Hajnorouzi, A.; Foruzan, A.H. A novel method for the estimation of the acoustic bubble radius distribution. *Measurement* **2020**, *154*, 107497. [CrossRef]
7. Nishida, Y.; Matsumura, T.; Ishii, K. Ultrasonic Cleaner using Two Transducers for Ship Hull Cleaning Robot. In Proceedings of the International Conference on Artificial Life and Robotics, Oita, Japan, 20–23 January 2020; ALife Robotics Corporation Ltd.: Oita, Japan, 2022; pp. 779–784. [CrossRef]
8. Srathonghuam, K.; Wonganu, B.; Busayaporn, W.; Thongsri, J. Vibration Analysis and Development of a Submersible Ultrasonic Transducer for an Application in the Inhibitory Activity of Pathogenic Bacteria. *IEEE Access* **2021**, *9*, 142362–142373. [CrossRef]
9. Phophayu, S.; Kliangklom, K.; Thongsri, J. Harmonic Response Analysis of Tank Design Effect on Ultrasonic Cleaning Process. *Fluids* **2022**, *7*, 99. [CrossRef]
10. Priya, S. Advances in energy harvesting using low profile piezoelectric transducers. *J. Electroceram.* **2007**, *19*, 165–182. [CrossRef]
11. Lin, S.; Xu, J. Effect of the Matching Circuit on the Electromechanical Characteristics of Sandwiched Piezoelectric Transducers. *Sensors* **2017**, *17*, 329. [CrossRef]
12. Wei, C.; Chen, H.; Chen, Y. Design of an automatic impedance matching circuit based on frequency tracking of ultrasonic transducer. In Proceedings of the 2020 IEEE 5th Information Technology and Mechatronics Engineering Conference, Chongqing, China, 12–14 June 2020.
13. Jin, Z.; Huo, L.; Long, T.; Guo, X.; Tu, J.; Zhang, D. An Online Impedance Analysis and Matching System for Ultrasonic Transducers. *IEEE Trans. Ultrason. Ferroelectr. Freq. Control* **2019**, *66*, 591–599. [CrossRef]
14. Jittakort, J.; Nimsontorn, J.; Sirboonrueng, B.; Chua-on, S.; Pinpathomrat, P.; Chudjuarjeen, S. A Class D Voltage Source Resonant Inverter for Ultrasonic Cleaning Application. In Proceedings of the 2018 International Conference on Engineering, Applied Sciences, and Technology, Phuket, Thailand, 4–7 July 2018.
15. Ebrahimi, R.; Ayobi, N.; Ghasemi, P.S.; Aghdam, E.N. Real-Time Control of Resonance Point of Piezoelectric Transducers Based on Class D Power Converter. In Proceedings of the 2019 27th Iranian Conference on Electrical Engineering, Yazd, Iran, 30 April–2 May 2019.
16. Jüschke, M.; Koch, C.; Dreyer, T. An erosion sensor based on a quartz crystal microbalance for quantitative determination of the cleaning efficiency in an ultrasonic vessel. *Ultrason. Sonochemistry* **2014**, *21*, 1900–1906. [CrossRef]
17. Xu, H.; Tu, J.; Niu, F.; Yang, P. Cavitation dose in an ultrasonic cleaner and its dependence on experimental parameters. *Appl. Acoust.* **2016**, *101*, 179–184. [CrossRef]
18. Tangsopa, W.; Keawklan, T.; Kesngam, K.; Ngaochai, S.; Thongsri, J. Improved design of ultrasonic cleaning tank using harmonic response analysis in ANSYS. In *IOP Conference Series: Earth and Environmental Science*; IOP Publishing: Bristol, UK, 2018.
19. Tangsopa, W.; Thongsri, J. Development of an industrial ultrasonic cleaning tank based on harmonic response analysis. *Ultrasonics* **2019**, *91*, 68–76. [CrossRef] [PubMed]
20. Shiiba, M.; Yahagi, M.; Morishita, T.; Okada, N.; Kurosawa, M.K.; Takeuchi, S. Development of Anti-Cavitation Hydrophone-Study on the Novel Hydrophone with New Cap Structure Titanium Front Plate. In Proceedings of the 2018 IEEE International Ultrasonics Symposium, Kobe, Japan, 22–25 October 2018.
21. Feng, H.; Yang, W. Ultrasonic processing. In *Nonthermal Processing Technologies for Food*; Wiley-Blackwell and IFT Press: Somerset, UK, 2011.
22. Sivakumar, V.; Mohan, R. Measurement and mapping of cavitation energy in leather and Material Processing vessels using an ultrasonic horn. *Appl. Phys. A* **2022**, *128*, 27. [CrossRef]
23. Eriksson, E. Characterization of Surface Defects Caused by Ultrasonic Cleaning of Aluminium. 2022. Available online: http://www.diva-portal.org/smash/get/diva2:1624472/FULLTEXT01.pdf (accessed on 17 November 2022).
24. Mason, T.J.; Lorimer, J.P. An introduction to sonochemistry. *Endeavour* **1989**, *13*, 123–128. [CrossRef]
25. Zhang, Y.; Dong, M.; Meng, Q.-D.; Cai, L. The topology analysing of a cascade multilevel class-D power amplifier. In Proceedings of the 2012 International Conference on Control Engineering and Communication Technology, ICCECT 2012, Shenyang, China, 7–9 December 2012; pp. 109–112. [CrossRef]
26. Cheng, H.L.; Cheng, C.A.; Fang, C.C.; Yen, H.C. Single-switch high-power-factor inverter driving piezoelectric ceramic transducer for ultrasonic cleaner. *IEEE Trans. Ind. Electron.* **2010**, *58*, 2898–2905. [CrossRef]
27. Yusof, N.S.M.; Babgi, B.; Alghamdi, Y.; Aksu, M.; Madhavan, J.; Ashokkumar, M. Physical and chemical effects of acoustic cavitation in selected ultrasonic cleaning applications. *Ultrason. Sonochem.* **2016**, *29*, 568–576. [CrossRef]
28. Wang, L.; Memoli, G.; Hodnett, M.; Butterworth, I.; Sarno, D.; Zeqiri, B. Towards a reference cavitating vessel Part III—Design and acoustic pressure characterization of a multi-frequency sonoreactor. *Metrologia* **2015**, *52*, 575–594. [CrossRef]
29. Wei, Z.; Weavers, L.K. Combining COMSOL modeling with acoustic pressure maps to design sono-reactors. *Ultrason. Sonochem.* **2016**, *31*, 490–498. [CrossRef]
30. Hodnett, M. *Measurement Techniques in Power Ultrasonics*; Elsevier Ltd.: Amsterdam, The Netherlands, 2015. [CrossRef]
31. Crawford, A.E. A Practical Introduction to Ultrasonic Cleaning. 1963. Available online: https://www.sciencedirect.com/science/article/abs/pii/0041624X63900568 (accessed on 18 November 2022).
32. Zhong, G.; Kang, M.; Yang, S. Precision obtained using an artificial neural network for predicting the material removal rate in ultrasonic machining. *Appl. Sci.* **2017**, *7*, 1268. [CrossRef]
33. Oinonen, M.; Laitinen, M.; Kyyrä, J. Current measurement and short-circuit protection of an IGBT based on module parasitics. In Proceedings of the 2014 16th European Conference on Power Electronics and Applications, Lappeenranta, Finland, 26–28 August 2014.

34. Yuan, B.; Jiang, Y.; Zhu, L. Study on the processing methods of aluminuim foil measurement signals for ultrasonic cleaning parameters. In Proceedings of the 2011 2nd International Conference on Digital Manufacturing and Automation, ICDMA 2011, Zhangjiajie, China, 5–7 August 2011; pp. 1180–1183. [CrossRef]
35. Lais, H.; Lowe, P.S.; Gan, T.H.; Wrobel, L.C. Numerical modelling of acoustic pressure fields to optimize the ultrasonic cleaning technique for cylinders. *Ultrason. Sonochem.* **2018**, *45*, 7–16. [CrossRef] [PubMed]
36. Tangsopa, W.; Thongsri, J. A Novel Ultrasonic Cleaning Tank Developed by Harmonic Response Analysis and Computational Fluid Dynamics. *Metals* **2020**, *10*, 335. [CrossRef]
37. Duran, F.; Teke, M. Design and implementation of an intelligent ultrasonic cleaning device. *Intell. Autom. Soft Comput.* **2018**, *1*, 441–449. [CrossRef]